18. Cazeau-Duroca, C.; Lyazidi, S. A.; Cambou, P.; Peirigua, A.; Cazeau, Ph.; Pesquer, M. *J. Phys. Chem.* **1989**, *93*, 2347.
19. Cukier, R. L. *J. Phys. Chem.* **1994**, *98*, 2377 and references therein.
20. Kim, Y.; Cheon, H. W.; Yoon, M.; Song, N. W.; Kim, D. *Chem. Phys. Lett.* **1997**, *264*, 673.
21. Kim, Y. H.; Cho, D. W.; Yoon, M.; Kim, D. *J. Phys. Chem.* **1996**, 100, 15670 and references therein.
22. Chou, Pi-Tai; Martinrz, M. L.; Cooper, W. C. *Chem. Phys. Lett.* **1992**, *198*, 188.
23. *The Merk Index of Chemicals and Drugs*, 12th Ed.; p 499.
24. Cho, D. W.; Kim, Y. H.; Kang, S. G.; Yoon, M.; Kim, D. *J. Phys. Chem.* **1994**, *98*, 558.
25. Shabestary, N.; EL-Bayoumi, M. A. *Chem. Phys. Lett.* **1984**, *106*, 107.
26. Joshi, H. C.; Mishra, H.; Tripathi, H. B. *J. Photochem. Photobiol.* **1997**, *105*, 15.

The Potential Energy Surfaces and Dipole Moment Functions of NH_2 by *ab initio* Effective Valence Shell Hamiltonian

Seung Hun Yun, YoungSok Yun, Jong Keun Park, and Hosung Sun*†

Department of Chemistry, Pusan National University, Pusan 609-735, Korea
†Department of Chemistry, SungKyunKwan University, Suwon 440-746 and Center for Molecular Science, KAIST, Taejon 305-701, Korea
Received June 26, 1998

The second order effective valence shell Hamiltonian (H^v), which is based on quasidegenerate many-body perturbation theory, is applied to determining the potential energy surfaces and the dipole moment functions of the various valence states of NH_2. The H^v calculated values are found to be in good agreement with those of other ab initio calculations or experiments. It signifies the fact that the H^v is a good *ab initio* method to describe the energies and properties of various valence states with a same chemical accuracy. Furthermore, it is shown that the lowest (second order for energy and the first order for property) order H^v method is very accurate for small molecules like NH_2 and the matrix elements of H^v which are computed only once are all we need to accurately describe all the valence states simultaneously.

Introduction

The quasidegenerate many-body perturbation theory (QDMBPT) is a Rayleigh-Schrödinger perturbation theory for quasidegenerate case. Here the quasidegeneracy means that states of interest are neither nondegenerate nor degenerate, rather the states lie very closely to each other in energy.[1-3] One of such quasidegeneracy may be found in valence electronic states of molecules. The effective valence shell Hamiltonian (H^v) theory is nonetheless the QDMBPT but the name comes from the fact that the quasidegenerate states are valence states. In H^v, the valence states are defined as states within valence space which is a small configuration state function space composed of prechosen valence orbitals. The reason why only valence space is considered in H^v is that the valence states are the most important states in chemistry. But the generality is not lost here because if one wants another states, say Rydberg states, one can easily expand the valence space to include whatever states of interest. The valence states in valence space may not be quasidegenerate. This problem is adequately solved in the effective valence shell Hamiltonian by giving a flexibility in defining the zeroth order Hamiltonian and molecular orbital energies. Therefore the H^v can be considered as the most rigorous quasidegenerate many-body perturbation theory.

H^v has been applied to various atoms,[4-6] many diatomics,[7-14] triatomics,[15,16] and polyenes.[17-22] Energy levels, excitation energies, ionization potentials, electron affinities, potential energy curves, transition dipole moments, oscillator strengths, and radiative transition probabilities are investigated using H^v.[7-14] For polyenes not only valence states but also Rydberg states as an example of intruder states are studied.[17-22] But for triatomics, except for the orbital structure change of BeH_2,[15,16] no applications of H^v have not been made yet.

In the present work we apply the second order H^v to determining the potential energy surfaces, relating quantities, and dipole moment functions of the valence states of NH_2. While several theoretical studies on NH_2 have been published,[23-31] not many experimental studies have been reported.[32-37] Among theoretical works Peyerimhoff *et al.*'s MRD-CI work is the most extensive so that it provides a good example to compare our H^v results with.[30] The purpose of the present work is to verify how well the effective valence shell Hamiltonian can reproduce the dipole properties as well as the valence state potential energy surfaces of triatomics with an example of NH_2. Therefore detailed analyses on the electronic structures of NH_2 are not presented, instead the focus lies on the nature

of H^v method itself.

In the following section, the introduction of H^v and its extended form for molecular property calculation is made. The detailed explanations on computational procedure and comparison of H^v results with other theoretical or experimental data follow. Conclusions are provided in the last section.

Theory

The full molecular Schrödinger equation is written as,

$$H\Psi = E\Psi \tag{1}$$

Now let $\{\phi\}$ be a complete set of all possible determinantal or configuration state functions within a given orbital basis set. Then Ψ may be expanded in this basis as,

$$\Psi = \sum_k C_k \phi_k \tag{2}$$

where $\{C_k\}$ is the set of expansion coefficients. Partitioning theory is now utilized to reexpress the Schrödinger equation (1) in terms of a subset of the expansion coefficients $\{C_k\}$.

Define a primary space, P, as containing some prechosen set, $\{\phi_i,\ i\in \mathrm{P}\}$, of all the configurations. The remaining functions, $\{\phi_j,\ j\in \mathrm{Q}\}$, form the secondary Q space. That is P + Q = 1. A full ab initio calculation involves all the configurations within P space along with a complementary set of configurations in Q space. The core, valence, and excited orbitals form a complete set of orbitals. The configuration state functions in Q space contain either excited orbitals and/or core to valence excitations.

The wavefunctions Ψ can be represented as a linear superposition of all possible determinantal functions,

$$\Psi = \sum_{i\in P} C_i \phi_i + \sum_{i\in Q} C_i \phi_i \tag{3}$$

We utilize a matrix representation where C_P designates the column vector of the expansion coefficients C_i for $i\in$ P, C_Q for those $j\in$ Q. The Schrödinger equation (1) can then be expressed in supermatrix form as,

$$\begin{bmatrix} H_{PP} & H_{PQ} \\ H_{QP} & H_{QQ} \end{bmatrix} \begin{bmatrix} C_P \\ C_Q \end{bmatrix} = E \begin{bmatrix} C_P \\ C_Q \end{bmatrix} \tag{4}$$

where $H_{PP} = \langle\phi_i | H | \phi_{i'}\rangle$ for $i,\ i'\in$ P denotes the sub-block of the Hamiltonian matrix within P space, $H_{PQ} = \langle\phi_i | H | \phi_j\rangle$ for $i\in$ P, $j\in$ Q that between P and Q, *etc.* Equation (4) is equivalent to the pair of coupled equations

$$H_{PP}C_P + H_{PQ}C_Q = EC_P \tag{5a}$$
$$H_{QP}C_P + H_{QQ}C_Q = EC_Q \tag{5b}$$

Rearranging (5b), we can formally solve this equation for C_Q to give

$$C_Q = (E1_Q - H_{QQ})^{-1} H_{QP}C_P \tag{6}$$

where 1_Q is the unit matrix in Q space, and the inverse matrix is taken solely within Q space. Substituting (6) into (5a) gives the well-known partitioned Hamiltonian,

$$H^v C_P \equiv [H_{PP} + H_{PQ}(E1_Q - H_{QQ})^{-1} H_{QP}]\ C_P = EC_P \tag{7}$$

which is the desired equation solely in the primary space P. Equation (7) involves the effective Hamiltonian, H^v, defined only in P space, and has eigenvalues E identical to those of the full Schrödinger equation (1).

With the aid of quasidegenerate many-body perturbation theory, we can expand (7) to obtain energy independent form of H^v. Let P be a valence space, which consists of all valence configuration state functions. The inverse matrix in equation (7) can be expanded with respect to a certain reference energy, E_0, to obtain an (equivalent) energy independent form of H^v. This proceeds by dividing the full Hamiltonian into two parts,

$$H = H_0 + V \tag{8}$$

where H_0 is the zeroth-order Hamiltonian (possibly a one-electron operator) and V is the perturbation. When H_0 is chosen to be a Fock operator, V represents the so called "correlation energy".

To obtain the practical form of H^v, the (8) can be projected onto the P. Then the resulting H^v is

$$H^v = PH_0P + PVP + PVQ(E_0 - H_0)^{-1} QVP + \cdots \tag{9}$$

where P is a projector onto P space and Q a projector onto Q space. Then, quasidegenerate many-body perturbation theory gives the second order approximation,

$$H^v = PHP + \frac{1}{2}\sum_{\Lambda,\Lambda'} [P(\Lambda)VQ(E_0 - H_0)^{-1} QVP(\Lambda') + h.c.] \tag{10}$$

where *h.c.* designates the Hermitian conjugate of the preceding term and $P(\Lambda)$ designates the projector onto the valence space basis function $|\Lambda\rangle$. The explicit details of the formulations are given in references 5 and 6. The present study utilizes only the second order expansion, where the denominators in the inverse matrix in (10) are taken as only the orbital energy contributions to diagonal matrix elements. H_{PP} in equation (4) or (7) includes all the valence configurations.

It can be shown that the (10) has matrix elements between determinantal functions which differ by 0, 1, 2, 3, $\cdots$, n_v valence shell orbitals, where n_v is the number of electrons in the valence shell, *i.e.*, in the P space. This, therefore, implies that the operator form of H^v cannot be represented solely in terms of one- and two-electron interactions, H_i^v and H_{ij}^v (molecular integral operators). In general H^v must contain three-, $\cdots$, n_v-electron operators,

$$H^v = E_C + \sum_{i=1}^{n} H_i^v + \frac{1}{2}\sum_{i\neq j=1}^{n} H_{ij}^v + \frac{1}{3!}\sum_{i\neq j\neq k=1}^{n} H_{ijk}^v + \cdots \tag{11}$$

where E_C is the core energy, H_{ijk}^v is a three-electron operator, *etc.* Suppose the $2a_1$, $1b_2$, $3a_1$, $1b_1$, $4a_1$, and $2b_2$ orbitals are chosen as the valence orbitals for NH_2, H^v only has matrix elements within a $2a_1$, $1b_2$, $3a_1$, $1b_1$, $4a_1$, and $2b_2$ basis. For example, the nonzero one-electron matrix elements are $\langle 2a_1 | H_i^v | 2a_1\rangle$, $\langle 1b_2 | H_i^v | 1b_2\rangle$, $\langle 3a_1 | H_i^v | 3a_1\rangle$, $\langle 1b_1 | H_i^v | 1b_1\rangle$, $\langle 4a_1 | H_i^v | 4a_1\rangle$, $\langle 2b_2 | H_i^v | 2b_2\rangle$, *etc.* Similarly the two-electron parts, H_{ij}^v, and three-electron parts, H_{ijk}^v, have matrix elements which do not vanish by molecular symmetry. Within the second order approximation of H^v, no four- and higher-electron interaction terms appear.

Note that, once the matrix elements of H_i^v, H_{ij}^v, H_{ijk}^v, $\cdots$,

have been evaluated, it is then a straightforward task to diagonalize H^v, to obtain all the valence state energies. Although H^v may have been evaluated through a calculation for one particular set of valence orbitals (*e.g.*, those valence orbitals could be chosen from the set of self-consistent field (SCF) orbitals for the ground state of the neutral molecule), the same H^v can be utilized for all charge states of the system (*i.e.*, the ions). It means that we do not need a separate ab initio calculation for each charge state. H^v is, in principle, exact for all these charge states, so if the primitive orbital basis is sufficiently good, H^v should represent them well provided the approximations in treating the Q space in equation (7) are not too severe.

Now we consider the property of molecule which can be represented with an operator A. The H^v can be extended to describing molecular properties. Consider an operator A whose diagonal and off-diagonal matrix elements between the normalized full space Ψ_i we desire. The matrix elements $\langle\Psi_i|A|\Psi_j\rangle$ may be transformed with quasidegenerate many-body perturbation theory into the matrix elements of an effective valence shell operator A^v between the orthonormal valence space effective eigenfunctions Ψ_i^v,

$$\langle\Psi_i|A|\Psi_j\rangle \equiv \langle\Psi_i^v|A^v|\Psi_j^v\rangle \quad (12)$$

Again, the specification that A^v be Hermitian and independent of the state Ψ_i leads to the lowest nontrivial order perturbative expansion,[5]

$$A^v = PAP + \sum_{\Lambda,\Lambda'} [P(\Lambda)VQ(E_0 - H_0)^{-1}QAP(\Lambda') + h.c.] \quad (13)$$

Thus, we may obtain the expectation values of A by first solving equation (7) and then by taking the corresponding matrix elements on the right-hand side of equation (12). The quasidegenerate many-body methods dispense with the numerical evaluation of the full space wavefunctions Ψ_i, so a new effective A^v must be evaluated for each operator A separately. However, once this A^v is obtained, it provides, in principle, all diagonal and off-diagonal matrix elements in the P space. One object of the present calculations is to determine whether all these matrix elements can be evaluated accurately from a perturbative truncation such as equation (13).

Either direct algebraic methods or many-body theory techniques can be used to reduce equation (13) to expressions for the matrix elements of A^v in the valence orbital basis. In the operator representation, A^v is,

$$A^v = A_c^v + \sum_{i=1}^{n_v} A_i^v + \frac{1}{2}\sum_{i\neq j=1}^{n_v} A_{ij}^v + \cdots \quad (14)$$

where A_c^v is the constant contribution from the core, A_i^v is a one-electron operator with matrix elements $\langle v|A_i^v|v'\rangle$ in the valence orbital basis $\{v\}$, *etc.* The original full space operator, A, may have one- and two-electron contributions, here we consider only the dipole operator which is one-electron operator. The close correspondence between equations (10) and (13) enables the straightforward determination of A^v from the formulas for the matrix elements of H^v. For dipole, $A = \sum_{i=1}^{n} er_i$ where e is an electronic charge, n is the number of total electrons, and r_i is a position vector for electron i. Nuclear contribution is separately calculated and added later following the Born-Oppenheimer approximation. A one-electron operator A generates two-electron effective valence space operators A_{ij}^v in the lowest nontrivial order specified by (13). This parallels the emergence of three-electron operator contributions in (11)[5,38].

The whole perturbation procedure is completely specified once the orbital basis and H_0 are chosen. Diagonalization of the perturbative H^v in the P valence space yields the valence state energies and eigenfunctions Ψ_i^v. The latter may then be employed along with (12) to calculate the expectation values of property operator A by use of the effective valence shell operator A^v.

Computations

A basis set is chosen as a set of contracted Gaussian functions. The (9s5p) basis set for nitrogen in the contraction [4s3p] as suggested by Dunning[24] was employed and augmented by one polarization d function with an exponent of 0.67,[25] one Rydberg s function with an exponent of 0.037[26] and one Rydberg p function with an exponent of 0.01.[26] The basis set for hydrogen consists of a (4s)/[2s] basis given by Dunning[24] and one polarization p function with an exponent of 1.08.[25]

With the prechosen basis set, the SCF calculations are performed for the ground $\tilde{X}^2B_1$ state ($1a_1^2\ 2a_1^2\ 1b_2^2\ 3a_1^2\ 1b_1^1$) of NH_2. We have to have molecular integrals and orbital energies in order to evaluate each H^v matrix elements. Molecular integrals are obtained from transforming integrals between basis functions with the SCF molecular orbital coefficients. The orbital energies are usually SCF orbital energies, that is, expectation values of Fock operator. The zeroth-order Hamiltonian H_0 is defined to be diagonal with orbital energies as diagonal elements. We used the SCF orbital energies in evaluating H^v matrix elements of NH_2. Orbital energies are taken from the diagonal elements of Fock operator of the ground $\tilde{X}^2B_1$ state of NH_2. To guarantee the fast convergence of the second order H^v, orbital energies for the valence orbitals are arithmetically averaged. The perturbative expansion of H^v always converges when both of the orbital energy gap between the highest core orbital and the lowest valence orbital and the orbital energy gap between the highest valence orbital and the lowest excited orbital are larger than the gap between the lowest and the highest valence orbital energies.

In H^v calculations, the valence space has to be predetermined and it consists of configuration state functions arising from $2a_1$, $1b_2$, $3a_1$, $1b_1$, $4a_1$, and $2b_2$ orbitals. This choice is appropriate because these orbitals mainly come from valence 2s and 2p orbitals of nitrogen and 1s orbitals of two hydrogens. The $1a_1$ molecular orbital consists predominantly of nitrogen 1s atomic orbital. Therefore the $1a_1$ orbital is considered as a core orbital where configuration is always $1a_1^2$. The $3a_1$ has N-H and H-H bonding character whereas the $1b_2$ has mainly N(in-plane 2p)-H and H-H antibonding character. The $1b_1$ is essentially the nitrogen 2p (out-of-plane) orbital. Low-lying virtual orbitals are the $4a_1$ and $2b_2$ orbitals, which are also from the nitrogen valence orbitals. Other higher-lying orbitals are

classified as excited orbitals. However, one should note that the H^v naturally includes all of core-core, core-valence and core-excited correlation, *etc.*

As shown in the theory section, H^v spans only within the valence space. In numerical calculations it means that we need to evaluate matrix elements of H^v only between valence orbitals to determine the valence state energies. In the previous H^v calculations it has been verified that the second order H^v contains most of electron correlations when small molecules like NH_2 are of interest. The corrections to the averaging first appear in the third order expansion H^v terms but we believe, from our experience, that these correction terms are small for small molecules like NH_2. So in the present work, we adopt the second order H^v formalism.

In H^v matrix element calculations, the core energy (E_c) is negative, one-electron matrix elements (H_i^v) are generally negative, but two-electron matrix elements (H_{ij}^v) are positive as expected. The three-electron matrix elements (H_{ijk}^v) are usually small. However, the neglect of those three-electron matrix elements give erroneous results in the valence state energies. Of course the diagonal H^v matrix elements are larger than the off-diagonal elements.

The NH_2 molecule is assumed to lie in the *yz* plane with the *z* axis taken to be collinear with the C_2 symmetry element in bent geometry. The whole H^v calculations have been repeated by changing internuclear distances (R_1, R_2) of the two N-H bonds and bond angle (θ) between HNH. The internuclear distances between N and H vary from 1.4 a.u. to 6.0 a.u. and the angle between HNH varies from 40° to 180°. The asymmetric variance of N-H internuclear distance, *i.e.*, two N-H distances (R_1, R_2) are different, is also performed.

The effective valence shell Hamiltonian formalism has been extended to treat operators for properties other than the valence state energies. The lowest order correlation corrections for the effective operators are analyzed for molecular properties corresponding to one-electron operators, and explicit computations were performed for the dipole moments of several low lying electronic states of NH_2.

The dipole operator in atomic unit is defined as

$$\mu = \sum_{\alpha} R_{\alpha} Z_{\alpha} - \underline{r} \tag{15}$$

whererm Z_α is the charge on the nucleus α at the position R_α, and $\underline{r}$ is the position operator for all electrons, $\underline{r} = \sum_{i=1}^{n} r_i$. The minus sign in (15) indicates a charge of electron. Within the Born-Oppenheimer approximation the nuclear contribution $\sum_{\alpha} R_{\alpha} Z_{\alpha}$ is constant for a given molecular geometry, and thus it is only necessary to evaluate the diagonal and off-diagonal matrix elements of the electronic position operator .

As in equation (12), to evaluate dipole moment (when A = $-\underline{r}$ and i is equal to j) we have to first calculate the effective wavefunction Ψ_i^v. It means that the H^v energy calculations must be performed before A^v calculations. Therefore the choice of basis set, valence orbitals, and orbital energies, *etc.* in A^v calculations should be identical with those in H^v energy calculations. The extra works in dipole moment calculations are evaluation of dipole integrals and of A^v matrix elements.

The dipole moment functions of NH_2 are calculated for the three lowest valence states with C_{2v} and C_s symmetry, respectively. The three lowest states are $\tilde{X}^2B_1$, $\tilde{A}^2A_1$, and $\tilde{B}^2B_2$ states which have been well studied before. The C_{2v} symmetry means that the two bond lengths between N and H are always equal and the bond angle of HNH is fixed (an equilibrium bond angle of NH_2) but N-H distance changes. The C_s symmetry means that the bond angle and one of the two N-H bond lengths are fixed (equilibrium values) but the two N-H distances are different from each other (*i.e.*, the other N-H distance changes). The internuclear distance between N and H varies from 1.4 a.u. to 6.0 a.u.

Results and Discussion

Potential Energy Surfaces. The results of the H^v calculations, *i.e.*, equilibrium geometry and state energies, are listed for the $\tilde{X}^2B_1$, $\tilde{A}^2A_1$, and $\tilde{B}^2B_2$ states in Table 1. The potential energy surfaces (C_{2v} symmetry) for the valence states are displayed in Figure 1 as a function of the HNH bond angle θ and the NH bond length R. As shown in Table 1, our results for the $\tilde{X}^2B_1$ and $\tilde{A}^2A_1$ states are in good agreement with experimental or other theoretical values. And the $\tilde{B}^2B_2$ state has not yet been determined spectroscopically but the comparison of our results with other theoretical values shows a reasonable agreement. We learn that the equilibrium geometries of the three states are quite different to each other. Furthermore Figure 1 indicates that the second order H^v calculations are accurate enough to determine potential energy surfaces of NH_2 and H^v method itself produces several state energies with same accuracy simultaneously.

The higher excited states are not much investigated before. To demonstrate the usefulness of H^v method we have calculated the potential energy surfaces of the next two excited states, *i.e.*, 2^2B_1 and 2^2A_1. Needless to say, we

Table 1. Equilibrium geometry and total energy for the lowest three states of NH_2 (C_{2v})

Method	R_e (Å)	θ (°)	Energy (au)
$\tilde{X}^2B_1$			
H^v	1.026	103.8	-55.866248
Full CI[a]	1.024	103.4	-55.742620
STO-3G[b]	1.058	100.2	
DZ*dp*CI[c]	1.029	103.1	-55.734051
MR-SDCI[d]	1.013	104.3	-55.749321
Expt.[e]	1.024	103.3	
$\tilde{A}^2A_1$			-55.816704
H^v	1.000	147.0	-55.688762
Full CI[a]	0.999	144.0	
STO-3G[b]	1.015	131.3	-55.680149
DZ*dp*CI[c]	0.999	143.4	
Expt.[e]	1.004±0.03	144±5	
$\tilde{B}^2B_2$			
H^v	1.138	50.0	-55.681858
DZ*d*CI[c]	1.184	46.8	-55.532042
DZ*dp*CI[c]	1.162	47.5	-55.557980
MRD-CI[d]	1.130	50.0	-55.602670

[a] Ref. 39. [b] Ref. 42. [c] Ref. 40. [d] Ref. 43. [e] Refs. 44, 45, and 46.

used the same matrix elements of H^v which were used to calculate the energies of lower valence states to evaluate the energies of these high lying states. The dominant configurations for the excited states of NH_2 are

$(1a_1)^2\ (2a_1)^2\ (2b_2)^2\ (3a_1)^1\ \ (1b_1)^1\ (4a_1)^1$ $\quad 2^2B_1$ state
$(1a_1)^2\ (2a_1)^2\ (2b_2)^2\ (3a_1)^2\ (4a_1)^1$ $\quad 2^2A_1$ state

Contrary to the lowest three valence states, the $4a_1$ orbital is occupied in the two states.

For the 2^2B_1 state, the equilibrium geometry and energy were computed to be $R_e = 1.148$ Å, $\theta = 180.0°$, and E = -55.645167 au. Other theoretical calculation (MC-CEPA) for the 2^2B_1 state also revealed that $\theta = 180.0°$, *i.e.*, NH_2 is linear.[29] For the 2^2A_1 state, $R_e = 1.042$ Å, $\theta = 110.0°$, and E = -55.616954 au. Other theoretical values are 105.0° (MC-CEPA)[29] and ≈100.0° (MRD-CI)[28] for the bond angle of HNH, respectively. Our H^v values are slightly different from other theoretical values, but experimental geometry is not known yet. The potential energy surfaces for these states are displayed in Figure 2 as a function of the HNH bond angle θ and the NH bond length R.

Dissociation and Excitation Energies. There may be two dissociation processes; one is $NH_2 \rightarrow N + H + H$ (C_{2v} symmetry), the other is $NH_2 \rightarrow NH + H$ (C_s symmetry). For the $NH_2 \rightarrow N + H + H$ (Figure 3) process, the H^v calculated

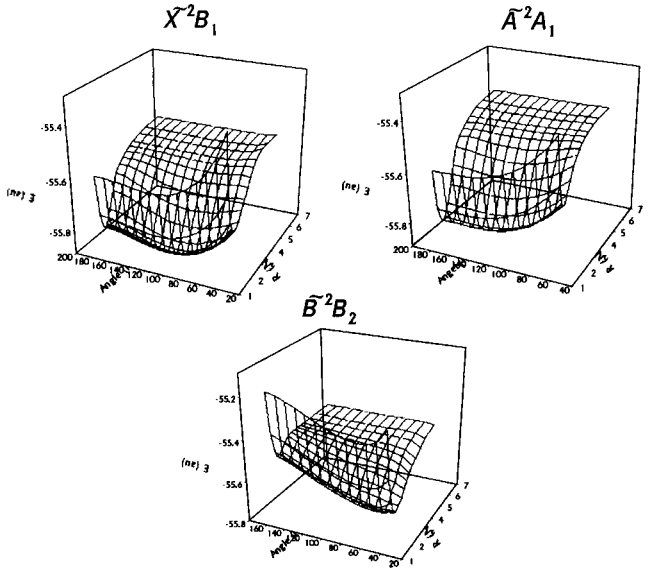

Figure 1. The potential energy surfaces for $\tilde{X}^2B_1$, $\tilde{A}^2A_1$ and $\tilde{B}^2B_2$ states of NH_2. Two NH bond lengths are always kept equal (C_{2v}).

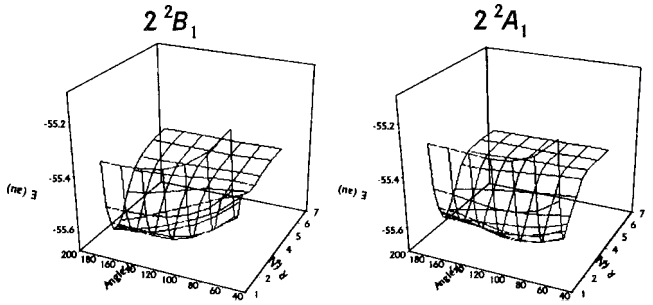

Figure 2. The potential energy surfaces for the 2^2B_1 and 2^2A_1 states of NH_2. Two NH bond lengths are always kept equal (C_{2v}).

dissociation energies, D_e are as follows.

$NH_2(\tilde{X}^2B_1) \rightarrow N(^4S) + H(^2S) + H(^2S)$ $\quad D_e = 8.92$ eV
$NH_2(\tilde{A}^2A_1) \rightarrow N(^2D) + H(^2S) + H(^2S)$ $\quad D_e = 10.24$ eV
$NH_2(\tilde{B}^2B_2) \rightarrow N(^2D) + H(^2S) + H(^2S)$ $\quad D_e = 6.56$ eV
$NH_2(2^2B_1) \rightarrow N(^4P) + H(^2S) + H(^2S)$ $\quad D_e = 6.62$ eV
$NH_2(2^2A_1) \rightarrow N(^2P) + H(^2S) + H(^2S)$ $\quad D_e = 5.85$ eV

For the $NH_2 \rightarrow NH + H$ (Figure 4) process, one H atom is far removed from the NH fragment and dissociation energy is calculated with the pseudodiatomic model (NH-H). The dissociation energies are;

$NH_2(1^2A'') \rightarrow NH(X^3\Sigma^-) + H(^2S)$ $\quad D_e = 4.75$ eV
$NH_2(1^2A') \rightarrow NH(a^1\Delta) + H(^2S)$ $\quad D_e = 4.57$ eV
$NH_2(2^2A') \rightarrow NH(b^1\Sigma^+) + H(^2S)$ $\quad D_e = 1.36$ eV
$NH_2(3^2A') \rightarrow NH(A^3\Pi) + H(^2S)$ $\quad D_e = 1.36$ eV

After overcoming a barrier of about 1.90 eV, the $2^2A''$ state energy drops down steeply to the dissociation products of $NH(a^1\Delta) + H(^2S)$. The reason for the barrier is probably a weak avoided crossing with higher-lying $^2A''$ states.[30]

To illustrate the dissociation process more clearly, the two dimensional potential energy curves are provided in Figures 3 and 4. In Figure 3, the HNH bond angle is fixed at its equilibrium value and the potential energy curve is drawn along the change of N-H bond length (The two N-H bond lengths are kept equal all the way). From the figure, we see that our H^v calculated potential curves are very smooth and lead to correct separate atom limits. Also the ordering of five states are correctly manifested. In Figure 4, another dissociation process is shown in terms of energy and geometry. The separate atom limits are NH + H. For the process, the dissociating enegies are smaller than that for N + H + H dissociation. The 2^2B_1 state ($2^2A''$ state in C_s symmetry) has a small energy barrier as mentioned before.

Not only the dissociation energies but also the excitation

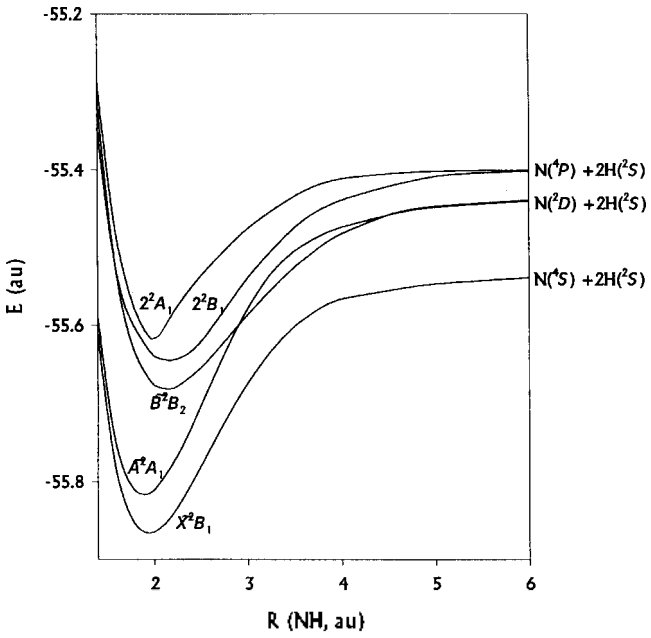

Figure 3. The potential energy curves for the five lowest-lying states of NH_2 dissociating into N + H + H at the equilibrium angle of HNH.

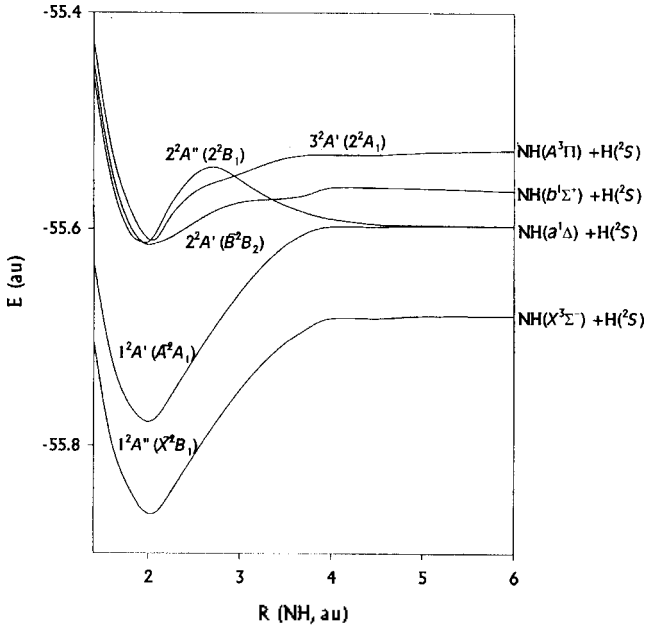

Figure 4. The potential energy curves for the five lowest-lying states of NH_2 as a function of one N-H bond length, keeping the other N-H distance and the bond angle fixed at the equilibrium values.

Table 2. Vertical excitation energy (eV)

	H^v	MRD-CI[a]	MRD-CI[b]
$\tilde{A}^2A_1 \leftarrow \tilde{X}^2B_1$	2.32	2.161	2.20
$\tilde{B}^2B_2 \leftarrow \tilde{X}^2B_1$	6.76	6.639	6.50
$2^2B_1 \leftarrow \tilde{X}^2B_1$	6.90	7.633	7.62
$2^2A_1 \leftarrow \tilde{X}^2B_1$	6.84	7.690	7.55

[a] Refs. 26 and 28. [b] Ref. 30.

energies can be determined from the full potential energy surfaces. Table 2 lists the vertical excitation energies between the ground $\tilde{X}^2B_1$ and the excited states. Vertical excitation energies are the state energy differences when the geometry of NH_2 is fixed at the initial state, *i.e.*, the ground $\tilde{X}^2B_1$ state. The energy differences between the minima of potential energy surfaces of two states are adiabatic excitation energies. The adiabatic excitation energies are also calculated and listed in Table 3. In the Tables we compare our H^v values with other available data and they are in good agreement to each other.

Overall the H^v method reproduces various dissociation and excitation energies for various valence states with a same accuracy. It is an advantage of H^v method and we prove the usefulness of H^v with its current application to NH_2.

Dipole Moment Functions. The dipole moments for

Table 3. Adiabatic excitation energy (eV)

	H^v	DZ*dp*CI[a]	MBPT[b]	Expt.[c]
$\tilde{A}^2A_1 \leftarrow \tilde{X}^2B_1$	1.45	1.47	1.41	1.40
$\tilde{B}^2B_2 \leftarrow \tilde{X}^2B_1$	5.02	4.79		
$2^2B_1 \leftarrow \tilde{X}^2B_1$	6.02			
$2^2A_1 \leftarrow \tilde{X}^2B_1$	6.98			

[a] Ref. 40. [b] Ref. 41. [c] Ref. 47.

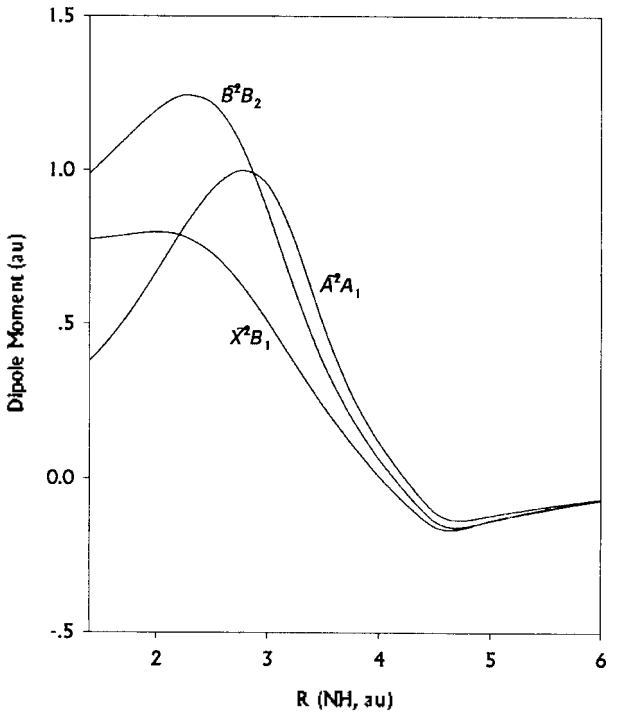

Figure 5. The dipole moment functions for the three valence states of NH_2 dissociating into N + H + H at the equilibrium angle of HNH.

the three lowest valence states as a function of internuclear distance of N-H are presented in Figure 5. The total dipole moments at equilibrium geometry are listed in Table 4. As shown in Table 4, our A^v values are in good agreement with other theoretical values, indicating that the second order H^v formalism combined with the first order A^v is accurate enough.

In Figure 5 ($NH_2 \rightarrow N + H + H$), the positive value indicates the polarity of $N^{\delta-}$ $2H^{\delta+}$. In the figure, the two N-H distances are always kept equal and the HNH bond angle is always fixed at equilibrium angle. At the range of small and medium R, the dipole moment is positive, which indicates

Table 4. Dipole moments for the lowest three states. R_e and θ are an equilibrium geometry at which dipole moment is evaluated

Method	R_e (Å)	θ (°)	Dipole
$\tilde{X}^2B_1$			
A^v	1.026	103.8	0.796
MGE[a]	1.080	101.8	0.720
DZ*d*[b]	1.014	104.8	0.840
DZ*dp*[b]	1.013	104.8	0.824
$\tilde{A}^2A_1$			
A^v	1.000	147.0	0.334
MGE[a]	1.040	133.6	0.323
DZ*d*[b]	0.992	140.9	0.348
DZ*dp*[b]	0.989	142.4	0.323
$\tilde{B}^2B_2$			
A^v	1.138	50.0	1.325
MGE[a]	1.620	26.5	0.354
DZ*dp*[b]	1.156	46.3	1.181

[a] Ref. 48. [b] Ref. 40.

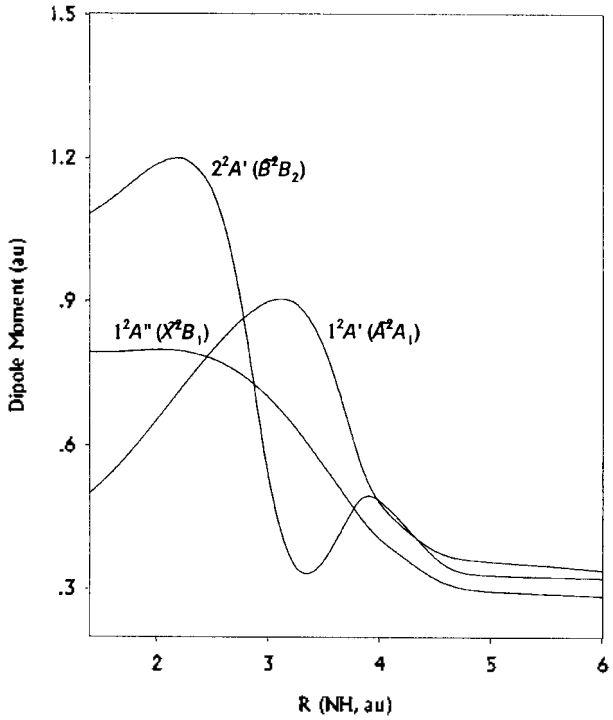

Figure 6. The dipole moments (z-component) for the three valence states of NH_2 as a function of one N-H bond length, keeping the other N-H distance and the bond angle fixed at the equilibrium values.

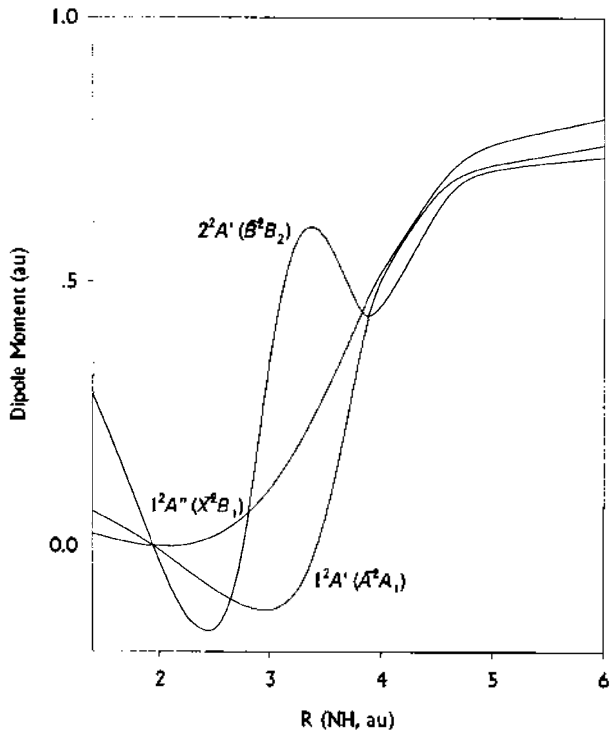

Figure 7. The dipole moments (y-component) for the three valence states of NH_2 as a function of one N-H bond length, keeping the other N-H distance and the bond angle fixed at the equilibrium values.

that the nitrogen atom has an negative end. As the bond distances become larger, the dipole moments of all the three states become negative where the redistribution of electrons occurs and the nitrogen becomes positive. This phenomenon is frequently found in small molecules.[31] As R becomes very large, the dipole moments reach to zero because at the separate atom limits, NH_2 is completely dissociated into neutral atoms (N, H, and H). Dipole moment is a vector property, *i.e.*, $\vec{\mu} = \mu_x\hat{x} + \mu_y\hat{y} + \mu_z\hat{z}$. In our coordinate system, μ_x is always zero because triatomic molecule (NH_2) is, of course, planar. When NH_2 has a C_{2v} symmetry, *i.e.*, two N-H bond lengths are equal, μ_y is also zero. So only μ_z component is nonzero and the dipole vector is along the z-axis. For C_{2v} case, we can always replace $\vec{\mu}$ with μ_z. Figure 5 shows the C_{2v} case.

In Figures 6 and 7, the dipole moment functions of the three states are shown for the process of $NH_2 \rightarrow NH + H$. In this case, the bond angle is fixed but the two N-H distances are different. When NH_2 has a C_s symmetry, *i.e.*, two N-H bond lengths are different, not only μ_z but also μ_y is nonzero. So the direction of $\vec{\mu}$ vector is in between $\hat{y}$ and $\hat{z}$ axis. For C_s case, $\vec{\mu}$ has two components and Figure 6 shows the μ_z component and Figure 7 shows the μ_y.

As shown in Figures 6 and 7, the behavior of dipole moment component with respect to N-H distance is rather complicated. Since other experimental or theoretical studies on this kind of dipole moment functions have not been reported, we can not assess the accuracy of our results. The physical meaning of dipole moment functions along this study should be investigated further. Figure 8 presents the magnitude of dipole moments, *i.e.*, $|\vec{\mu}| = \sqrt{\mu_y^2 + \mu_z^2}$. The direction of $\vec{\mu}$ changes as R varies so that it is difficult to present the dipole moment vector in a form of figure. From the figure, we can, at least, verify that, at very large R distance, the magnitude of NH_2 dipole moment becomes

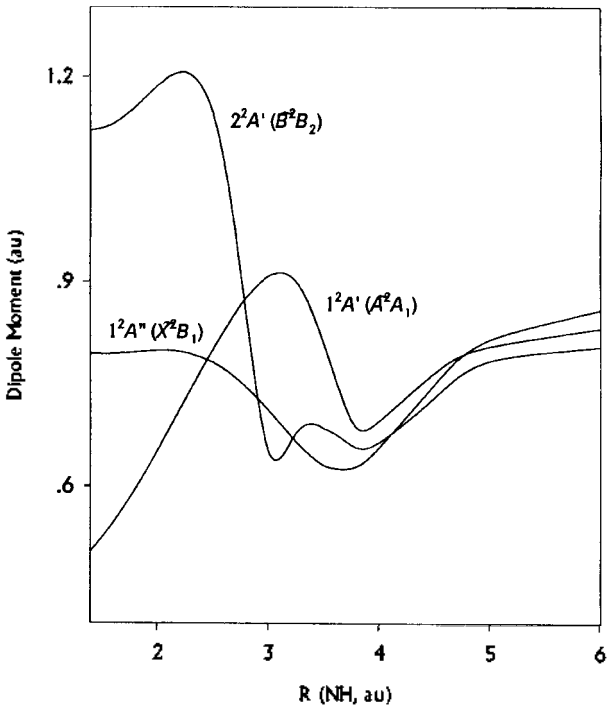

Figure 8. Magnitude of dipole moments for the three valence states of NH_2 as a function of one N-H bond length, keeping the other N-H distance and the bond angle fixed at the equilibrium values.

equal to that of NH molecule, as expected. From a single A^v calculation for dipole moments, the transition dipole moments are also simultaneously computed but they are not reported in the present article.

Conclusions

The potential energy surfaces of NH_2 molecular system have been determined using the ab initio second order effective valence shell Hamiltonian method. Since the H^v is defined within a valence space, the same H^v matrix elements were used to determine all valence states. The three-electron matrix elements are found to be important in evaluating valence state energies accurately.

The overall structure of the calculated potential energy surfaces for various states of NH_2 have been reproduced accurately and they are in good agreement with those of other ab initio calculations. It indicates that the H^v method includes the electron correlations properly.

The extended effective valence shell Hamiltonian formalism (A^v) to treat operators for properties other than valence state energies is relatively new method. The dipole moments of NH_2 system have been determined as a function of internuclear distances using the lowest order effective Hamiltonian A^v method. It is noted once again that one set of A^v matrix elements at a given geometry yields the dipole moments for all the valence states of NH_2 and this feature of the method greatly reduces the computational effort. Our computed dipole moments are also in reasonable agreement with other theoretical values.

The current work strongly indicates that A^v, *i.e.*, the effective valence shell Hamiltonian for property, is as efficient and accurate as H^v energy method. In summary, using the H^v and A^v method, we have determined the many valence electronic structures of NH_2 very accurately.

Acknowledgment. This work was supported by Center for Molecular Science, MOST-FOTD, and Ministry of Education (BSRI-97-3409), Korea.

References

1. Iwata, S.; Freed, K. F. *Chem. Phys. Lett.* **1974**, *28*, 176.
2. Westhaus, P.; Bradford, E. G. *J. Chem. Phys.* **1975**, *63*, 5416.
3. Bradford, E. G.; Westhaus, P. *J. Chem. Phys.* **1976**, *64*, 4276.
4. Yeager, D. L.; Sun, H.; Freed, K. F.; Herman, M. F. *Chem. Phys. Lett.* **1978**, *57*, 490; Lee, Y. S.; Sun, H.; Sheppard, M. G.; Freed. K. F. *J. Chem. Phys.* **1980**, *73*, 1472.
5. Sun, H.; Freed, K. F.; Herman, M. F.; Yeager, D. L. *J. Chem. Phys.* **1980**, *72*, 4158; Sun, H.; Freed, K. F. *J. Chem. Phys.* **1988**, *88*, 2659.
6. Sheppard, M. G.; Freed, K. F. *J. Chem. Phys.* **1981**, *75*, 4507.
7. Wang, X. C.; Freed, K. F. *J. Chem. Phys.* **1989**, *91*, 3002.
8. Sun, H.; Freed, K. F. *Chem. Phys. Lett.* **1981**, *78*, 531.
9. Park, J. K.; Sun, H. *Bull. Korean Chem. Soc.* **1990**, *11*, 34.
10. H. Sun, *Bull. Korean Chem. Soc.* **1988**, *9*, 101.
11. Sun, H.; Lee, Y. S.; Freed, K. F. *Chem. Phys. Lett.* **1988**, *150*, 529.
12. Takata, T.; Sheppard, M. G.; Freed, K. F. *J. Chem. Phys.* **1983**, *79*, 352.
13. Takata, T.; Freed, K. F. *J. Chem. Phys.* **1984**, *80*, 3696.
14. Andersson, K.; Malmqvist, P.-A.; Roos, B. O. *J. Chem. Phys.* **1992**, *96*, 1218.
15. Wang, X. C.; Freed, K. F. *J. Chem. Phys.* **1989**, *91*, 1142.
16. Hoffmann, M. R.; Wang, X. C.; Freed, K. F. *Chem. Phys. Lett.* **1987**, *136*, 392.
17. Martin, C. H.; Freed, K. F. *J. Chem. Phys.* **1994**, *101*, 4011.
18. Graham, R. L.; Freed, K. F. *J. Chem. Phys.* **1992**, *96*, 1304.
19. Martin, C. H.; Graham, R. L.; Freed, K. F. *J. Chem. Phys.* **1993**, *99*, 7833.
20. Martin, C. H.; Freed, K. F. *J. Chem. Phys.* **1994**, *100*, 7454.
21. Martin, C. H.; Graham, R. L.; Freed, K. F. *J. Phys. Chem.* **1994**, *98*, 3467.
22. Lee, Y. S.; Freed, K. F.; Sun, H.; Yeager, D. L. *J. Chem. Phys.* **1983**, *79*, 3862; Martin, C. H.; Freed, K. F. *J. Phys. Chem.* **1995**, *99*, 2701; *J. Chem. Phys.* **1994**, *101*, 5929; Lee, S. Y.; Freed, K. F. *J. Chem. Phys.* **1996**, *104*, 3260; Chaudri, R. K.; Mudholkar, A.; Freed, K. F.; Martin, C. H.; Sun, H. *J. Chem. Phys.* **1997**, *106*, 9252.
23. Harris, R. A. *J. Chem. Phys.* **1967**, *49*, 3967.
24. Dunning, Jr., T. H. *J. Chem. Phys.* **1970**, *53*, 2823.
25. Neisius, D.; Verhaegen, G. *Chem. Phys. Lett.* **1982**, *89*, 228.
26. Saxon, R. P.; Lengsfield, B. H.; Liu, B. *J. Chem. Phys.* **1983**, *78*, 312.
27. Lykos, P. G.; Parr, R. G. *J. Chem. Phys.* **1956**, *24*, 1166.
28. Peyerimhoff, S. D.; Buenker, R. J. *Can. J. Chem.* **1979**, *57*, 3182.
29. Biehl, H.; Schonnenbeck, G.; Stuhl, F.; Staemmler, V. *J. Chem. Phys.* **1994**, *101*, 3819.
30. Vetter, R.; Zulicke, L.; Koch, A.; van Dishoeck, E. F.; Peyerimhoff, S. D. *J. Chem. Phys.* **1996**, *104*, 5558.
31. Lie, G. C.; Hinze, J.; Liu, B. *J. Chem. Phys.* **1973**, *59*, 1887.
32. Tonooka, M.; Yamamoto, S.; Kobayashi, K.; Saito, S. *J. Chem. Phys.* **1997**, *106*, 2563.
33. Gibson, S. T.; Greene, J. P.; Berkowitz, J. *J. Chem. Phys.* **1985**, *83*, 4319.
34. Halpern, J. B.; Hancock, G.; Lenzi, M.; Welge, K. H. *J. Chem. Phys.* **1975**, *63*, 4808.
35. Kroll, M. *J. Chem. Phys.* **1975**, *63*, 319.
36. Amano, T.; Kawaguchi, K.; Kakimoto, M.; Saito, S.; Hirota, E. *J. Chem. Phys.* **1982**, *77*, 159.
37. Mayama, S.; Hiraoka, S.; Obi, K. *J. Chem. Phys.* **1984**, *80*, 7.
38. Sun, H.; Sheppard, M. G.; Freed, K. F. *J. Chem. Phys.* **1981**, *74*, 6842.
39. Bauschlicher Jr., C. W.; Langhoff, S. R.; Talyor, P. R.; Handy, N. C.; Knowles, P. J. *J. Chem. Phys.* **1986**, *85*, 1469.
40. Bell, S.; Schaefer III, H. F. *J. Chem. Phys.* **1973**, *67*,

5173.
41. Cole, S. J.; Bartlett, R. J. *J. Chem. Phys.* **1987**, *86*, 873.
42. Lathan, W. A.; Hehre, W. J.; Curtiss, L. A.; Pople, J. A. *J. Am. Chem. Soc.* **1971**, *93*, 6377.
43. Pople, J. A.; Luke, B. T.; Frisch, M. J.; Binkley, J. S. *J. Phys. Chem.* **1985**, *89*, 2198.
44. Herzberg, G.; Ramsey, D. A. *J. Chem. Phys.* **1952**, *20*, 347; Herzberg, G.; Ramsey, D. A. *Discuss. Faraday Soc.* **1953**, *14*, 11.
45. Herzberg, G. *Electronic Spectra of Polyatomic Molecules*, Van Nostrand, Princeton, 1967.
46. Dressler, K.; Ramsey, D. A. *J. Chem. Phys.* **1957**, *27*, 971.
47. Jungen, Ch.; Hallin, K.-E. J.; Merer, A. J. *Mol. Phys.* **1980**, *40*, 25.
48. Brown, R. D.; Williams, G. R. *Mol. Phys.* **1973**, *25*, 673.

PM3 Studies on the Acid-Catalyzed Hydrolysis of 1-Phenoxyethyl Propionate

Chan Kyung Kim*, In Young Lee, Dong Soo Chung, Bon-Su Lee, and Ikchoon Lee

Department of Chemistry, Inha University Inchon 402-751, Korea
Received June 26, 1998

Acid catalyzed hydrolysis of 1-phenoxyethyl propionate, **I**, has been studied using the PM3 method in the gas phase. The first step of the reaction is the protonation of basic sites, three different oxygens in **I**, producing three protonated species **II**, **III** and **IV**. All possible reaction pathways have been studied from each protonated structure. Changes in the reaction mechanisms have also been discussed from the results obtained by varying a nucleophile from a water monomer to a water dimer to a complex between one water molecule and an intermediate product (propionic acid or phenol) produced in the preceding unimolecular dissociation processes. Minimum energy reaction pathway is 2-W among the possible pathways, in which water dimer acts as an active catalyst and therefore facilitates the formation of a six-membered cyclic transition state. Lower barrier of 2-W is ascribed to an efficient bifunctional catalytic effect of water molecules. PM3-SM3.1 single point calculations have been done at the gas-phase optimized structure (SM3.1/PM3//PM3) to compare theoretical results to those of experimental work.

Introduction

Alkanoates have two special functional groups, ester and actetal, and the hydrolysis of the alkanoates has been studied extensively due to the mechanistic importance of this compound as an intermediate of the enzymic reactions.[1] Mechanistic studies on the hydrolysis of alkanoates have been done experimentally under the acidic, basic, and neutral conditions.[2] Especially, hydrolysis reactions of ester functional group in acidic or basic condition are known to be fast and these are classified into 8 different reaction mechanisms.[3] Under the acidic condition, the reaction is classified into two different modes - acyl and alkyl bond cleavages. The reactions are classified as $A_{AC}1$ or $A_{AC}2$ in the former case, and as $A_{AL}1$ or $A_{AL}2$ in the latter case depending on the number of molecule involved in the rate determining steps.

R. A. McClelland reported that the unimolecular mechanism is favorable in the case of acyclic system from the studies on the hydrolysis of cyclic and acyclic systems.[4] R. A. Cox and K. Yates proposed an A-1 mechanism from the ρ values obtained by varying the concentration of acid under the dilute acid.[5]

Recently C. D. Hall and C. W. Goulding carried out an experimental study on the acid-catalyzed hydrolysis of 1-aryloxyethyl alkanoates (see eq. 1).[6] Products of the reaction are a carboxylic acid, an aldehyde and an alcohol.

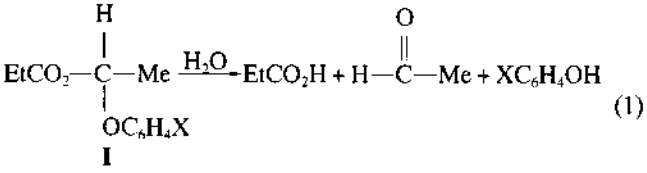

(1)

I

In their study, reaction mechanism was interpreted from the rate constants obtained under strong acidic (low pH) and strong basic (high pH) conditions and substituent effects of aryl ring and ^{18}O labelling experiments.[7] The reactions are proposed to proceed through different mechanisms depending on the pH of the reaction medium. In acidic region, the reaction proceeds through an A-1 mechanism (A_{AL}-1) involving predissociation of a carbonium ion and subsequent attack by water. In basic condition, the mechanism is $B_{AC}2$ and in the neutral region, the reaction is $A_{AC}2$ mechanism which involves a nucleophilic attack of water molecule to the carbonyl group.[8-15]

In this study, computational method was used to interpret the complex mechanism of 1-phenoxyethyl alkanoate, **I**. In basic media, a tetrahedral intermediate can be easily formed by the addition of hydroxide ion to the carbonyl group without reaction barrier, and this mechanism has been

*Author to whom correspondence should be addressed.